Quantum theory of multiwave mixing. I. General formalism

Murray Sargent III and David A. Holm
Optical Sciences Center, University of Arizona, Tucson, Arizona 85721

M. Suhail Zubairy
Institute for Modern Optics, Department of Physics and Astronomy, University of New Mexico, Albuquerque, New Mexico 87131
and Department of Physics, Quaid-i-Azam University, Islamabad, Pakistan
(Received 6 July 1984; revised manuscript received 19 November 1984)

We present a theory that describes how one strong classical wave and one or two weak quantum-mechanical waves interact in a nonlinear two-level medium. The analysis is applicable to several popular problems with and without cavities. In particular, the theory treats laser and optical bistability instabilities, predicting when the instabilities grow from spontaneous emission. The theory is a multimode extension of Scully-Lamb theory that derives the equations that describe population pulsations, combination tones, mode locking, resonance fluorescence, Rayleigh scattering, and phase conjugation with quantum-mechanical fields. Hence the theory both presents new results on instabilities and phase conjugation, and also unifies the treatment of a variety of phenomena in the context of Lamb theory. The present paper (first of the series) presents the basic formalism, leaving most applications to subsequent papers in this series. The following paper presents equivalent derivations based on a purely operator formalism.

I. INTRODUCTION

A basic question in laser physics is, can side modes build up in the presence of a single cw oscillating mode, that is, is single-mode operation stable? This question has been studied since the early 1960's. In fact multimode operation was easily found to occur in lasers with inhomogeneous broadening and/or standing waves, since different cavity modes interact at least in part with different groups of atoms.[1] Predictions also were made that a sufficiently intense single mode of a homogeneously broadened unidirectional ring laser[2-6] or an optical bistability (OB) cavity[7] leads to multimode operation. Two kinds of laser instabilities could occur, one for which three frequencies would grow with distinct wavelengths (multiwave-length instability) and one for which induced anomalous dispersion allows three frequencies to correspond to the same wavelength. Haken[8] showed the single-wave length instability could be chaotic, while Graham[9] showed the multiwavelength case could be chaotic. Hendow and Sargent[10] showed that these instabilities are due to the dynamic Stark effect or equivalently, to population pulsations. The population pulsations induced by the multimode field scatter energy from the intense mode into side modes. This produces the side-mode gain that causes single-frequency operation to be unstable. One- and two-side-mode gain and/or absorption coefficients have been derived by a number of people.[11-16] Casperson[17] predicted and observed a single-wavelength instability in the inhomogeneously broadened Xe laser, where he attributed the induced anomalous dispersion to spectral hole burning. Hendow and Sargent[10] showed that population pulsations can be equally important. Later work has shown how to treat these instabilities including detuning of the large mode. The Casperson instability is readily observed,[17-19] and yields the first all-optical generator of chaos.[19]

In spite of the fact that the buildup of side modes relies on spontaneous emission to occur, virtually all theories of these effects have been semiclassical. Lugiato and coworkers[20] have discussed fluorescence spectra for a single mode in a cavity using a quantized field, but did not consider side modes. Reid and Walls have treated quantized signal and conjugate waves in degenerate four-wave mixing.[21] The present paper gives a detailed derivation of the first fully quantal theory[22] that gave equations predicting that the side modes build up from spontaneous emission, and that gave the general coefficients for the quantized coupled-mode equations in four-wave mixing. From studying the three-peaked spectrum induced by a strong field in resonance fluorescence, one would expect that the spontaneous emission spectrum for laser side modes would also have Rabi sidebands resulting from the Rabi modulation of the upper-level population. This is the case, but the spectrum is substantially altered due to four-wave mixing in the medium.

Our theory is a multimode extension of the Scully-Lamb theory[23] of the laser and derives the quantized-field version of the population pulsations and combination tones introduced in Lamb's semiclassical laser theory.[24] It gives the basis for a fully quantal discussion of phase conjugation, and shows how mode-locking concepts can be incorporated into the single-mode Scully-Lamb theory.[23] Aspects of the theory reduce to the two-mode, three-level problem treated by Singh and Zubairy.[25] The two-mode special case also provides a new way of describing resonance fluorescence and resonant Rayleigh scattering.[26-29]

A parallel calculation using purely operator formalism is presented by Stenholm *et al.*[30] in the following paper. The semiclassical absorption coefficient and single-side-mode coefficients are well known in the literature. Since the present paper derives for the first time the corresponding two-side-mode case needed for cavity instabilities and phase conjugation, it is desirable to have an independent calculation of these results. The purely operator formalism has advantages in providing a well-defined recipe for obtaining all terms to second order in the weak modes. Background semiclassical calculations[16] are compared to the present calculations in the course of the derivations.

Section II presents a three-level version of the single-mode theory of Scully and Lamb[23] in a form that is most easily extended to the side-mode cases. Two of the levels are involved in the laser transitions, and the third level is connected to the others by level decays and pumps. This model can reduce to the upper- to ground-state lower-level problem usually considered in resonance fluorescence and ruby lasers, and yet can also describe interactions with two excited states. The single-atom coarse-grained time rate of change used by Scully and Lamb is replaced by a density matrix analysis more closely paralleling the semiclassical theory.

Section III develops the basic analysis for the single-side-mode laser case, revealing the quantum form of the population pulsations. It derives the equation of motion for the side-mode photon number, recovering the semiclassical gain coefficient and finding the spontaneous emission term that leads to side-mode buildup. Section IV reduces the formulas to two popular two-level configurations: one with a ground lower state often used in laser spectroscopy, and one with an excited lower state, typically found in lasers.

Section V introduces the second side mode, symmetrically placed in frequency on the other side of the strong mode. With the help of the strong mode, each side mode induces population pulsations that influence the other side mode in the form of quantum combination tones. We use density-matrix equations of motion to find a reduced side-mode density operator equation of motion, from which various expectation values can be calculated. In particular, we recover the semiclassical coupled-mode equations for the complex electric-field amplitudes and derive the equations of motion for the side-mode photon numbers.

Explicit spectra predicted by the theory for resonance fluorescence in cavities, laser side-mode buildup, and phase conjugation have been given in Ref. 22, and more detailed illustrations will be presented in subsequent papers.

II. SINGLE-MODE EQUATIONS OF MOTION

In this section, we derive the single-mode Scully-Lamb theory equations in a form suitable for our multimode extensions. To be able to treat both upper- to ground-state transitions as well as transitions between excited states, we consider the three-level system depicted in Fig. 1 The field modes of interest cause transitions between levels a and b while level c acts as a reservoir connected to a and b by level decays and pumps. γ_a and γ_b are the rates at which levels a and b decay to level c, and Λ_a and Λ_b are the pumping rates from level c to levels a and b. Γ describes the decay from level a to level b. By setting $\gamma_a=\gamma_b=0$, we recover the two-level upper- to ground-state problem. Although level decays from a and b to the same level typically cannot both be electric-dipole allowed, nonradiative processes can produce these decays. More complicated level schemes do not change the form of our equations, and lead only to somewhat more complicated coefficients. In an interaction picture, our single-mode Hamiltonian has the form (in rad/sec)

$$H=(\omega-\nu)\sigma_z+[gaU(\mathbf{r})\sigma^\dagger+\text{H.c.}] \tag{1}$$

plus terms describing decay (resulting from Weisskopf-Wigner and other relevant reservoir interactions). Here a is the field-mode annihilation operator, U_j is the corresponding spatial mode factor, σ and σ_z are the atomic spin-flip and probability-difference operators, ω and ν are the atomic and field frequencies, respectively, and g is the atom-field coupling constant.

The components of the atom-field density operator ρ are given by $\rho_{an,an}=\langle an\,|\,\rho\,|\,an\rangle$, etc. Using the density operator equation of motion

$$\dot\rho=-i[H,\rho]+\cdots , \tag{2}$$

where the ellipsis represents the relaxation and pumping terms, and we find the equations of motion of the components to be

$$\dot\rho_{an,an}=-(\gamma_a+\Gamma)\rho_{an,an}+\Lambda_a\rho_{cn,cn}-(iV_{an,bn+1}\rho_{bn+1,an}+\text{c.c.}) , \tag{3}$$

$$\dot\rho_{bn+1,bn+1}=-\gamma_b\rho_{bn+1,bn+1}+\Gamma\rho_{an+1,an+1}+\Lambda_b\rho_{cn+1,cn+1}+[iV_{an,bn+1}\rho_{bn+1,an}+\text{c.c.}] , \tag{4}$$

$$\dot\rho_{an,bn+1}=-[\gamma+i(\omega-\nu)]\rho_{an,bn+1}+iV_{an,bn+1}(\rho_{an,an}-\rho_{bn+1,bn+1}) , \tag{5}$$

$$\dot\rho_{cn,cn}=\gamma_a\rho_{an,an}+\gamma_b\rho_{bn,bn}-(\Lambda_a+\Lambda_b)\rho_{cn,cn} , \tag{6}$$

where γ is the dipole decay constant often written as $1/T_2$, and $V_{an,bn+1}=gU\sqrt{n+1}$. Note that while (3)—(6) look semiclassical, they describe fully quantized transitions between atom-field levels. In addition we have the trace condition

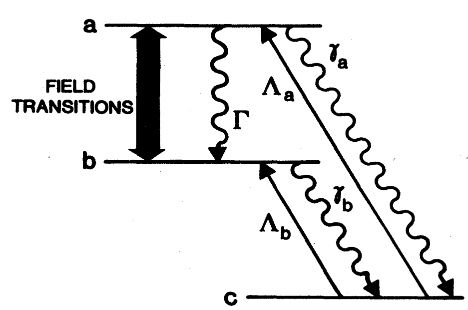

FIG. 1. Three-level atomic-energy level scheme that treats both purely excited-state interactions as well as upper- to ground-lower-state interactions in a uniform way.

$$\rho_{nn}=\sum_{\alpha}\rho_{an,an} \; . \tag{7}$$

As in semiclassical Lamb theory and in Scully-Lamb theory we suppose that the atoms react quickly compared to variations in the mode amplitudes. Hence we can solve Eqs. (3)–(6) in steady state by setting the time rates of change equal to zero. We eliminate $\rho_{cn,cn}$ in Eq. (3) and $\rho_{an+1,an+1}$ in Eq. (4) by using Eqs. (6) and (7) as follows. Solving Eq. (7) for $\rho_{cn,cn}$ and substituting $\rho_{bn,bn}$ from the steady-state solution of Eq. (6), we have

$$\begin{aligned}\rho_{cn,cn}&=\rho_{nn}-\rho_{an,an}-\rho_{bn,bn}\\&=\rho_{nn}-\rho_{an,an}\\&\quad+[\gamma_a\rho_{an,an}-(\Lambda_a+\Lambda_b)\rho_{cn,cn}]/\gamma_b\\&=\frac{\gamma_b\rho_{nn}-\rho_{an,an}(\gamma_b-\gamma_a)}{\gamma_b+\Lambda_a+\Lambda_b} \; .\end{aligned} \tag{8}$$

Similarly,

$$\begin{aligned}\rho_{an+1,an+1}&=\rho_{n+1,n+1}-\rho_{bn+1,bn+1}-\rho_{cn+1,cn+1}\\&=\rho_{n+1,n+1}-\rho_{bn+1,bn+1}-\frac{\gamma_a\rho_{an+1,an+1}+\gamma_b\rho_{bn+1,bn+1}}{\Lambda_a+\Lambda_b}\\&=\frac{(\Lambda_a+\Lambda_b)\rho_{n+1,n+1}-\rho_{bn+1,bn+1}(\gamma_b+\Lambda_a+\Lambda_b)}{\gamma_a+\Lambda_a+\Lambda_b} \; .\end{aligned} \tag{9}$$

The steady-state solution to the dipole equation (5) is

$$\rho_{an,bn+1}=iV_{an,bn+1}D(\omega-\nu)(\rho_{an,an}-\rho_{bn+1,bn+1}) \; , \tag{10}$$

where the complex Lorentzian denominator

$$D(\omega-\nu)=1/[\gamma+i(\omega-\nu)] \; . \tag{11}$$

Substituting Eqs. (8) and (10) into Eq. (3) and solving for steady-state ($\dot{\rho}_{an,an}=0$), we find

$$\rho_{an,an}=N_a\rho_{nn}-\frac{(n+1)R}{2T_1\gamma_a'}(\rho_{an,an}-\rho_{bn+1,bn+1}) \; , \tag{12}$$

where the unsaturated probability of being in the upper level

$$N_a=\frac{\Lambda_a\gamma_b}{\gamma_a\gamma_b+\gamma_a\Lambda_b+\gamma_b\Lambda_a+\Gamma(\gamma_b+\Lambda_a+\Lambda_b)} \; , \tag{13}$$

the upper-level effective decay constant

$$\gamma_a'=\gamma_a+\Gamma+\frac{\Lambda_a(\gamma_b-\gamma_a)}{\gamma_b+\Lambda_a+\Lambda_b} \; , \tag{14}$$

the rate constant

$$R=4\,|gU|^2T_1T_2L(\omega-\nu) \; , \tag{15}$$

the probability difference decay time

$$T_1=\frac{1}{2}\left[\frac{1}{\gamma_a'}+\frac{1}{\gamma_b'}\right] , \tag{16}$$

and the dimensionless Lorentzian

$$L(\omega-\nu)=\gamma^2/[\gamma^2+(\omega-\nu)^2] \; . \tag{17}$$

Similarly substituting Eqs. (9) and (10) into Eq. (4), we find

$$\begin{aligned}\rho_{bn+1,bn+1}&=N_b\rho_{n+1,n+1}\\&\quad+\frac{(n+1)R}{2T_1\gamma_b'}(\rho_{an,an}-\rho_{bn+1,bn+1}) \; ,\end{aligned} \tag{18}$$

where

$$N_b=\frac{(\Lambda_a+\Lambda_b)\Gamma+\gamma_a\Lambda_b}{\gamma_a\gamma_b+\gamma_a\Lambda_b+\gamma_b\Lambda_a+\Gamma(\gamma_b+\Lambda_a+\Lambda_b)} \; , \tag{19}$$

$$\gamma_b'=\gamma_b+\frac{\Gamma(\gamma_b+\Lambda_a+\Lambda_b)+\Lambda_b(\gamma_a-\gamma_b)}{\gamma_a+\Lambda_a+\Lambda_b} \; . \tag{20}$$

Combining Eqs. (12) and (18), we find the probability difference

$$\rho_{an,an}-\rho_{bn+1,bn+1}=\frac{N_a\rho_{nn}-N_b\rho_{n+1,n+1}}{1+(n+1)R} \; . \tag{21}$$

Substituting Eq. (21) into (10), we have the complex electric-dipole term

$$\rho_{an,bn+1}=iV_{an,bn+1}D(\omega-\nu)\left[\frac{N_a\rho_{nn}-N_b\rho_{n+1,n+1}}{1+(n+1)R}\right] . \tag{22}$$

Substituting the equations of motion (2), (4), and (6) into the time rate of change of Eq. (7), we find the single-mode field equation of motion

$$\begin{aligned}\dot{\rho}_{nn}&=(-iV_{an,bn+1}\rho_{bn+1,an}\\&\quad+iV_{an-1,bn}\rho_{bn,an-1})+\text{c.c.}\end{aligned} \tag{23}$$

Note that although this was derived for the three-level scheme in Fig. 1, Eq. (23) is also valid for an arbitrary number of reservoir levels like c. Inserting Eq. (22) and including the standard $\nu/2Q$ loss terms used in Scully-Lamb theory,[24,1] we have

$$\begin{aligned}\dot{\rho}_{nn}&=-\frac{(n+1)R}{2T_1}\left[\frac{N_a\rho_{nn}-N_b\rho_{n+1,n+1}}{1+(n+1)R}\right]\\&\quad+\frac{nR}{2T_1}\left[\frac{N_a\rho_{n-1,n-1}-N_b\rho_{n,n}}{1+nR}\right]\\&\quad+\frac{\nu}{2Q}\rho_{n+1,n+1}-\frac{\nu}{2Q}\rho_{nn} \; .\end{aligned} \tag{24}$$

Equation (24) reduces to the original Scully-Lamb[23] photon-number equation of motion if we set the upper- to lower-level decay rate $\Gamma=0$ and $\Lambda_b=0$, which give $N_b=0$. Equation (24) also describes upper- to lower-level decay schemes, and with appropriate modification of the N_a and N_b factors, it describes other pumping and decay schemes. To be consistent with our assumption that the field varies little in the atomic lifetimes, the cavity loss constant $\nu/2Q$ must be small compared to atomic decay constants or the fields must have reached a steady state. Note that nonlinear dispersion is included in this equation of motion and that the field amplitude is assumed to be uniform throughout the cavity.

For use in the two- and three-mode interactions that follow, the strong mode at frequency ν_2 is treated classically, that is, the difference between n_2 and n_2+1 is ignored. In this approximation, we need explicit values for the semiclassical probabilities ρ_{aa} and ρ_{bb}. To this end, we set

$$(n+1)R \simeq nR = 4n\,|gU|^2 T_1 T_2 L_2 = I_2 L_2 \,, \tag{25}$$

where L_2 is a special case of the dimensionless Lorentzian

$$L_n = \frac{\gamma^2}{\gamma^2+\Delta_n^2}\,, \tag{26}$$

and $\Delta_n = \omega - \nu_n$. Combining Eqs. (25) and (21) with (12) and tracing over the field index n, we have the semiclassical probabilities

$$\rho_{aa} = N_a - \frac{I_2 L_2}{2T_1\gamma_a'}\frac{N_a - N_b}{1+I_2L_2} = \frac{f_a}{1+I_2L_2}\,, \tag{27}$$

where the upper-level probability factor

$$f_a = \left[1+\frac{I_2L_2}{2T_1\gamma_b'}\right]N_a + \frac{I_2L_2}{2T_1\gamma_a'}N_b\,. \tag{28}$$

Similarly,

$$\rho_{bb} = \frac{f_b}{1+I_2L_2}\,, \tag{29}$$

where

$$f_b = \frac{I_2L_2}{2T_1\gamma_b'}N_a + \left[1+\frac{I_2L_2}{2T_1\gamma_a'}\right]N_b\,. \tag{30}$$

Note that $f_a - f_b = N_a - N_b$. In this semiclassical approximation, the electric dipole element (22) becomes

$$\rho_{ab} = iV_{ab}D(\omega-\nu_2)\frac{N_a-N_b}{1+I_2L_2}\,. \tag{31}$$

III. SINGLE-SIDE-MODE INTERACTION WITH EXCITED-STATE ATOMS

In general our approach consists of using a reduced three-mode atom-field density matrix in generalization of the single-mode matrix in Sec. II. Our Hamiltonian (in rad/sec) has the form, in an interaction picture rotating at the strong field frequency ν_2,

$$H = (\omega-\nu_2)\sigma_z + \sum_{j=1}^{3}[(\nu_j-\nu_2)a_j^\dagger a_j + (g a_j U_j \sigma^\dagger + \text{H.c.})] \tag{32}$$

plus terms describing decay (resulting from Weisskopf-Wigner and other relevant reservoir interactions). Here a_j is the annihilation operator for the jth field mode, $U_j = U_j(r)$ is the corresponding spatial mode factor, σ and σ_z are the atomic spin-flip and probability-difference operators, ω and ν_j are the atomic and field frequencies, respectively, and g is the atom-field coupling constant. The rotating-wave approximation has been made. The field modes have the distribution shown in Fig. 2. In this section we consider one classical strong mode at frequency ν_2 and one weak fully quantal side mode at frequency ν_1. The two-level atom interacting with two fields involves at least four atom-field levels. We limit the analysis to the four in Fig. 3 by assuming the side mode at frequency ν_1 cannot by itself saturate the atomic response. As for the semiclassical theories,[2–11,13–16] the strong mode at frequency ν_2 can be arbitrarily intense. Note that the unperturbed (undressed) atom-field states are used, rather than dressed atoms. This leads to population pulsations rather than to level splitting. Background semiclassical calculations to guide and compare with are reviewed by Sargent.[16]

To derive the photon rate equation for mode 1, we need the density matrix elements for the four levels in Fig. 3 along with the six off-diagonal elements connecting the levels. The states depicted in Fig. 3 have been numerically labeled as shown for notational simplicity. For example, the matrix element ρ_{51} is equal to $\langle a n_1 n_2 | \rho | b n_1+1 n_2 \rangle$. The ρ_{41} and ρ_{52} dipole terms and the level probabilities ρ_{55} and ρ_{11} are easily found from the semiclassical treatment, as demonstrated later. In addition, the four levels are coupled by relaxation and decay processes to the lower level c. Just as in the single-mode case we write equations of motion for the remaining elements using the standard density matrix equation of motion (2), here with the Hamiltonian of Eq. (32) summed from $j=1$ to $j=2$. This gives a-b elements

$$\dot\rho_{11} = -\gamma_b\rho_{11} + \Gamma\rho_{55} + \Lambda_b\rho_{c10,c10} + [(iV_{51}\rho_{15} + iV_{41}\rho_{14}) + \text{c.c.}]\,, \tag{33}$$

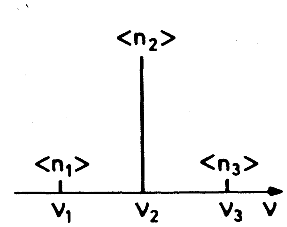

FIG. 2. Three-mode spectrum used for multiwave mixing such as in laser and/or optical-bistability instability studies, saturation spectroscopy, and phase conjugation.

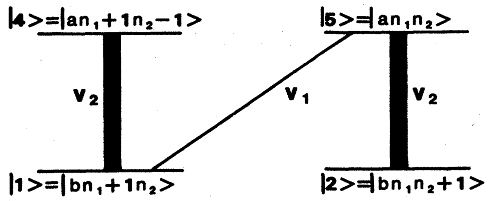

FIG. 3. Four-level atom-field energy-level scheme valid for two-mode interactions. Extra levels enter with three modes as shown in Fig. 4.

$$\dot{\rho}_{55} = -(\gamma_a + \Gamma)\rho_{55} + \Lambda_a \rho_{c00,c00} - [(iV_{51}\rho_{15} + iV_{52}\rho_{25}) + \text{c.c.}] , \tag{34}$$

$$\dot{\rho}_{51} = -(\gamma + i\Delta_1)\rho_{51} + iV_{51}(\rho_{55} - \rho_{11}) + i\rho_{54}V_{41} - iV_{52}\rho_{21} , \tag{35}$$

$$\dot{\rho}_{54} = -(\gamma_a + \Gamma + i\Delta)\rho_{54} + \Lambda_a \rho_{c01,c10} - i(V_{51}\rho_{14} - \rho_{51}V_{14} + V_{52}\rho_{24}) , \tag{36}$$

$$\dot{\rho}_{21} = -(\gamma_b + i\Delta)\rho_{21} + \Gamma\rho_{54} + \Lambda_b \rho_{c01,c10} + i(\rho_{25}V_{51} - V_{25}\rho_{51} + \rho_{24}V_{41}) , \tag{37}$$

$$\dot{\rho}_{24} = -(\gamma - i\Delta_3)\rho_{24} - iV_{25}\rho_{54} + i\rho_{21}V_{14} , \tag{38}$$

where

$$\Delta_n = \omega - \nu_n ,$$

$$V_{51} = gU_1\sqrt{n_1+1} ,$$

$$V_{52} = gU_2\sqrt{n_2+1} ,$$

and

$$V_{41} = gU_2\sqrt{n_2} .$$

These equations treat both modes quantum mechanically, except for the $\Gamma\rho_{55}$, $\Gamma\rho_{54}$, and $\gamma_b\rho_{21}$ contributions to Eqs. (33), (37), and (40), respectively. In these contributions we explicitly ignore the difference between n_2 and n_2+1, i.e., we treat the strong mode classically. In solving the equations we make this approximation uniformly throughout, specifically setting $V_{41} = V_{52} = V_2$. Keeping mode 2 quantum mechanical up to this point allowed us to write the equations of motion down correctly using Eq. (2). For simplicity we set $V_1 = V_{51}$.

Equations (34) and (36) are coupled to c level elements $\rho_{c00,c00}$ and $\rho_{c01,c10}$, respectively, where for typographical simplicity, we write $c01$ for cn_1,n_2+1, and $c10$ for c,n_1+1,n_2. These c level elements have the equations of motion

$$\dot{\rho}_{c00,c00} = \gamma_a\rho_{55} + \gamma_b\rho_{b00,b00} - (\Lambda_a + \Lambda_b)\rho_{c00,c00} , \tag{39}$$

$$\dot{\rho}_{c01,c10} = \gamma_a\rho_{54} + \gamma_b\rho_{21} - (i\Delta + \Lambda_a + \Lambda_b)\rho_{c01,c10} . \tag{40}$$

Note that this model does not use dressed states and that the simultaneous solution of Eqs. (33)–(40) automatically includes all possible ordering schemes of large and small interactions. In this way the successive decays using dressed states as discussed by Smithers and Freedhoff[31] are accounted for by our method.

The elements ρ_{54} and ρ_{21} correspond to the semiclassical population pulsations represented by d_1 of Sec. 2.2 of Ref. 16. They have the time dependence $e^{i\Delta t}$, where $\Delta = \nu_2 - \nu_1$. The element ρ_{42} is a polarization at frequency ν_3 induced by three (or more) photon processes involving combinations of ν_1 and ν_2 interactions. It corresponds to p_3 in Sec. 2.2 in Ref. 16.

In addition to the equations of motion, we have the general trace condition

$$\rho_{ij,mn} = \sum_\alpha \rho_{\alpha ij,\alpha mn} . \tag{41}$$

In particular for $\rho_{n_1,n_2+1;n_1+1,n_2} = \rho_{0110}$, we find

$$\rho_{0110} = \rho_{54} + \rho_{21} + \rho_{c01,c10} . \tag{42}$$

Here the ρ_{54} contribution once again ignores the difference between n_2 and n_2+1. Similarly to the single-mode case of Eq. (3), we combine the trace condition (42) with the steady-state solution to Eq. (40) to eliminate $\rho_{c01,c10}$ in Eq. (36). We find

$$\rho_{c01,c10} = \frac{\gamma_b\rho_{0110} - (\gamma_b - \gamma_a)\rho_{54}}{\gamma_b + \Lambda_a + \Lambda_b + i\Delta} , \quad = \frac{\gamma_a\rho_{0110} + (\gamma_b - \gamma_a)\rho_{21}}{\gamma_a + \Lambda_a + \Lambda_b + i\Delta} .$$

Substituting the first of these into Eq. (36) and solving for steady state, we find

$$\rho_{54} = \frac{\Lambda_a\gamma_b\rho_{0110}D_a'}{\gamma_b + \Lambda_a + \Lambda_b + i\Delta} - iD_a'(V_1\rho_{14} - \rho_{51}V_2^* + V_2\rho_{24}) , \tag{43}$$

where the complex D_a' factor is given by

$$D_a' = \frac{\gamma_b + \Lambda_a + \Lambda_b + i\Delta}{(\gamma_b + i\Delta)(\gamma_a + i\Delta) + \Lambda_a(\gamma_b + i\Delta) + \Lambda_b(\gamma_a + i\Delta) + (\gamma_b + \Lambda_a + \Lambda_b + i\Delta)\Gamma} . \tag{44}$$

Similarly combining Eqs. (42) and (40) to eliminate ρ_{54} in Eq. (37), we find the steady-state solution

$$\rho_{21} = \frac{[(\Lambda_a + \Lambda_b + i\Delta)\Gamma + \gamma_a\Lambda_b]D_b'\rho_{0110}}{\gamma_a + \Lambda_a + \Lambda_b + i\Delta} + iD_b'[\rho_{25}V_1 - V_2^*\rho_{51} + \rho_{24}V_2] , \tag{45}$$

where

$$D_b' = \frac{\gamma_a + \Lambda_a + \Lambda_b + i\Delta}{(\gamma_b + i\Delta)(\gamma_a + i\Delta) + \Lambda_a(\gamma_b + i\Delta) + \Lambda_b(\gamma_a + i\Delta) + (\gamma_b + \Lambda_a + \Lambda_b + i\Delta)\Gamma} . \tag{46}$$

The trace condition (41) also provides the equations of motion for the two field quantities of interest, the probability of n_1 photons, $p_{n_1} \equiv \rho_{n_1 n_1}$, and the field coherence function ρ_{0110}. Differentiating Eq. (41) for ρ_{0000} with respect to time, and substituting Eqs. (33), (34), and (39), we find

$$\dot{p}_{n_1} = \dot{\rho}_{55} + \dot{\rho}_{11} \,|_{n_1 \to n_1 - 1} + \dot{\rho}_{c00,c00}$$
$$= [iV_1^* \rho_{51} - i(V_1^* \rho_{51}) \,|_{n_1 \to n_1 - 1}] + \text{c.c.} \tag{47}$$

This equation allows us to calculate the resonance fluorescence spectrum and the build up of a laser side mode from quantum noise. All we need to find is the dipole element ρ_{51}. Note that although this was derived for the three-level scheme in Fig. 1, it is valid for arbitrary pumping and relaxation processes, that is, other levels to and from which decays and pumping occur do not change the validity of Eq. (47). It is similar in form to the single-mode equation of motion (23), but involves a more complicated calculation.

Similarly taking the time rate of change of Eq. (42) and substituting Eqs. (35), (36), and (40), we have the field coherence ρ_{0110} equation of motion

$$\dot{\rho}_{0110} = \dot{\rho}_{54} + \dot{\rho}_{21} + \dot{\rho}_{c01,c10}$$
$$= -i\Delta \rho_{0110} - iV_1(\rho_{14} - \rho_{25}) \ . \tag{48}$$

Here we have neglected the difference between n_2 and n_2+1. As shown below, this result yields the elastic (Rayleigh) portion of the scattering spectrum and like Eq. (47) is independent of the relaxation and/or pumping scheme. We solve this equation in steady state as

$$\rho_{0110} = -\frac{iV_1(\rho_{14} - \rho_{25})}{i\Delta} \ , \tag{49}$$

where the dipole elements ρ_{14} and ρ_{25} are given by Eq. (51). Here Δ typically has a size on the order of the atomic decay constants which cause the atomic response to equilibrate rapidly in comparison with the field transients. As $\Delta \to 0$, this approximation breaks down when the time $1/\Delta$ is comparable to the times over which the field varies. For a steady-state atom-field interaction, this leads to the delta-function spectrum associated with Rayleigh scattering as discussed following Eq. (67).

To solve the remaining equations, we note that the weak side-mode field assumption means that V_1 can only appear to second order. This means that the probabilities ρ_{55}, ρ_{44}, ρ_{22}, and ρ_{11} appearing in the equations of motion can be factored into the corresponding semiclassical value determined by the V_2 interactions alone [ρ_{aa} or ρ_{bb} from Eqs. (29) and (30)], multiplied by the probability of having n_1 or n_1+1 photons. Specifically, we have

$$\rho_{55} = \rho_{aa} p_{n_1}$$
$$= \frac{f_a}{1 + I_2 L_2} p_{n_1} \ , \tag{50a}$$

$$\rho_{11} = \frac{f_b}{1 + I_2 L_2} p_{n_1 + 1} \ , \tag{50b}$$

where we set $p_{n_1} \equiv \rho_{n_1 n_1}$ for typographical simplicity. Similarly the dipole elements ρ_{41} and ρ_{52} are

$$\rho_{52} = iV_2 D_2 \left[\frac{N_a - N_b}{1 + I_2 L_2} \right] p_{n_1}$$
$$= iV_2 D_2 d_{052} \ , \tag{51a}$$

$$\rho_{41} = iV_2 D_2 \left[\frac{N_a - N_b}{1 + I_2 L_2} \right] p_{n_1 + 1}$$
$$= iV_2 D_2 d_{041} \ , \tag{51b}$$

where D_2 is the ν_2 case of the complex Lorentzians

$$D_n = \frac{1}{\gamma + i(\omega - \nu_n)} \ . \tag{52}$$

Substituting Eq. (51) into Eq. (49), we have the field coherence function

$$\rho_{0110} = -\frac{V_1 V_2^* D_2^* (d_{041} - d_{052})}{i\Delta} \ . \tag{53}$$

We solve Eqs. (35) through (38) in steady state. Solving first for the dipole moments in Eqs. (35) and (38), we have

$$\rho_{51} - iD_1(V_1 d_{051} + V_2 d_{154}) \ , \tag{54}$$

$$\rho_{24} = -iD_3^* V_2^* d_{154} \ , \tag{55}$$

where from Eqs. (50)

$$d_{051} = \rho_{55} - \rho_{11} \tag{56}$$
$$= \frac{1}{1 + I_2 L_2} (f_a p_{n_1} - f_b p_{n_1 + 1}) \ ,$$

$$d_{154} = \rho_{54} - \rho_{21} \ . \tag{57}$$

Compare ρ_{51} to p_1 in the semiclassical theory [Ref. 23 Eq. (39)]. Similarly, ρ_{42} corresponds to p_3 of Ref. 23 Eq. (41). As for Ref. 23 Eq. (45), we substitute these dipole elements into the upper-level population pulsation equation (43) to find

$$\rho_{54} = \frac{\Lambda_a \gamma_b D_a' \rho_{0110}}{\gamma_b + \Lambda_a + \Lambda_b + i\Delta} - D_a' V_2^* [V_1 D_2^* d_{041} + D_1(V_1 d_{051} + V_2 d_{154}) + D_3^* V_2 d_{154}] \ . \tag{58}$$

This is almost identical to Ref. 23 Eq. (45), but here the V_1's include factors like $\sqrt{n_1+1}$ and the d_{041} and d_{051} include different initial photon-number probabilities. Similarly,

$$\rho_{21} = \frac{[(\Lambda_a + \Lambda_b + i\Delta)\Gamma + \gamma_a \Lambda_b] D_b' \rho_{0110}}{\gamma_a + \Lambda_a + \Lambda_b + i\Delta} + D_b' V_2^* [V_1 D_2^* d_{052} + D_1(V_1 d_{051} + V_2 d_{154}) + D_3^* V_2 d_{154}] \ . \tag{59}$$

Subtracting Eq. (59) from (58), solving for d_{154}, and substituting Eq. (49) for ρ_{0110}, we have

$$d_{154}=\rho_{54}-\rho_{21}$$
$$=-\frac{V_1V_2^*[2T_1F'd_{051}D_1+(D_a'+S/i\Delta)d_{041}D_2^*+(D_b'-S/i\Delta)d_{052}D_2^*]}{1+I_2F'\frac{\gamma}{2}(D_1+D_3^*)}\,, \tag{60}$$

where the complex dimensionless population pulsation factor

$$F'(\Delta)=\frac{1}{2T_1'}[D_a'(\Delta)+D_b'(\Delta)]\,, \tag{61}$$

and the scattering factor

$$S(\Delta)=\frac{\Lambda_a\gamma_b-\gamma_a\Lambda_b-(\Lambda_a+\Lambda_b+i\Delta)\Gamma}{(\gamma_a+i\Delta)(\gamma_b+i\Delta)+(\gamma_a+i\Delta)\Lambda_b+(\gamma_b+i\Delta)\Lambda_a+(\gamma_b+\Lambda_a+\Lambda_b+i\Delta)\Gamma}\,. \tag{62}$$

Substituting Eq. (60) into Eq. (54), we find

$$\rho_{51}=iD_1V_1\left[d_{051}-\frac{I_2\frac{\gamma}{2}\left[F'd_{051}D_1+\frac{D_2^*}{2T_1}[(D_a'+S/i\Delta)d_{041}+(D_b'-S/i\Delta)d_{052}]\right]}{1+I_2F'\frac{\gamma}{2}(D_1+D_3^*)}\right]. \tag{63}$$

For the limit of upper to ground-state lower-level decay, Eq. (60) is almost the same as the semiclassical Eq. (46) of Ref. 23, except for the way the d_0's enter (and the $\sqrt{n_1+1}$ factors in the V_1's),

$$\dot{p}_{n_1}=-(n_1+1)[A_1p_{n_1}-(B_1+\nu/2Q_1)p_{n_1+1}]+n_1[A_1p_{n_1-1}-(B_1+\nu/2Q_1)p_{n_1}]+\text{c.c.}\,, \tag{64}$$

where the coefficients

$$A_1=\frac{g^2D_1}{1+I_2L_2}\left[f_a-\frac{I_2\frac{\gamma}{2}[f_aF'D_1+(N_a-N_b)D_2^*(D_b'-S/i\Delta)/2T_1]}{1+I_2F'\frac{\gamma}{2}(D_1+D_3^*)}\right], \tag{65}$$

$$B_1=\frac{g^2D_1}{1+I_2L_2}\left[f_b-\frac{I_2\frac{\gamma}{2}[f_bF'D_1-(N_a-N_b)D_2^*(D_a'+S/i\Delta)/2T_1]}{1+I_2F'\frac{\gamma}{2}(D_1+D_3^*)}\right], \tag{66}$$

and where $\nu/Q_1=$cavity loss for mode 1.

Equation (64) has a straightforward physical interpretation. Each term can be understood in terms of the probabilities that the atoms make transitions resulting in the emission or absorption of a mode 1 photon. For example, (the absorption rate from an n_1+1 photon field + the cavity loss rate)$\times$(the probability of n_1+1 photons) is given by

$$(B_1+B_1^*+\nu/Q_1)(n_1+1)p_{n_1+1}$$

The A_1 coefficient is proportional to the population of level a and involves spontaneous and stimulated emissions, whereas the B_1 coefficient is proportional to the population of level b and involves absorptions. We are primarily interested in the buildup of mode 1, which can be described by the average photon number $\langle n_1\rangle=\sum_{n_1}n_1p_{n_1}$. Using Eq. (64), we find the equation of motion

$$\frac{d}{dt}\langle n_1\rangle=-A_1(\langle n_1^2\rangle+\langle n_1\rangle)-(B_1+\nu/2Q_1)\langle n_1^2\rangle+(B_1+\nu/2Q_1)(\langle n_1^2\rangle-\langle n_1\rangle)+A_1(\langle n_1^2\rangle+2\langle n_1\rangle+1)+\text{c.c.}$$
$$=(A_1-B_1-\nu/2Q_1)\langle n_1\rangle+A_1+\text{c.c.} \tag{67}$$

In the limit $\nu/2Q_1\gg B_1-A_1$, the photon rate Eq. (67) reduces to $d\langle n_1\rangle/dt=-\nu/2Q_1\langle n_1\rangle+A_1+\text{c.c.}$ In steady state, this gives the spontaneous emission spectrum $\langle n_1\rangle=(A_1+A_1^*)Q_1/\nu$. For an upper to lower-level decay scheme and large pump intensity, this leads to the standard three-peaked spectrum of resonance fluorescence. Note that the term proportional to $S/i\Delta$ leads to a contribution proportional to $i/\Delta+\text{c.c.}$ in Eq. (67). This gives the delta-function spectrum of resonant Rayleigh scattering.

Similarly, the two-mode coefficient A_1-B_1 yields the standard semiclassical two-mode gain and/or absorption coefficient.[11,13] For this fairly general three level scheme, we have

$$A_1 - B_1 = \frac{g^2 D_1 (N_a - N_b)}{1 + I_2 L_2} \left[1 - \frac{I_2 \frac{\gamma}{2} F'(D_1 + D_2^*)}{1 + I_2 F' \frac{\gamma}{2}(D_1 + D_3^*)} \right] . \tag{68}$$

IV. SIMPLE SINGLE-SIDE-MODE INTERACTION CASES

In considering absorptive optical bistability and resonance fluorescence, one usually treats transitions between the ground state and some excited state. This case is described by setting $\gamma_a = \gamma_b = 0$, which gives $T_1 = 1/\Gamma$. In this limit,

$$\Gamma D_a = \Gamma D_b = F = -S = \Gamma/(\Gamma + i\Delta) , \tag{69}$$

and $N_a = 0$, $N_b = 1$, $f_a = I_2 L_2 / 2$, $f_b = 1 + f_a$. Hence the coefficients A_1 and B_1 reduce to

$$A_1 = \frac{g^2 D_1}{1 + I_2 L_2} \left[\frac{I_2 L_2}{2} - \frac{I_2 \frac{\gamma}{2} F[D_1 I_2 L_2 / 2 - D_2^*(1 + \Gamma / i\Delta)/2]}{1 + I_2 F \frac{\gamma}{2}(D_1 + D_3^*)} \right] , \tag{70}$$

$$B_1 = \frac{g^2 D_1}{1 + I_2 L_2} \left[1 + \frac{I_2 L_2}{2} - \frac{I_2 \frac{\gamma}{2} F[(1 + I_2 L_2 / 2) D_1 + D_2^*(1 - \Gamma / i\Delta)/2]}{1 + I_2 F \frac{\gamma}{2}(D_1 + D_3^*)} \right] . \tag{71}$$

These values agree with Mollow's results.[26]

The excited-state laser limit considered in Ref. 22 is also of interest. This is given by the values

$$\Gamma = 0; \ \Lambda_a, \Lambda_b \ll \gamma_a, \gamma_b . \tag{72}$$

Here the pump constants are taken to be small compared to the decay constants since the rates $\gamma_\alpha \rho_{\alpha\alpha} \simeq \Lambda_\alpha \rho_{cc}$, and the reservoir probability $\rho_{cc} \gg \rho_{\alpha\alpha}$. These choices imply

$$\gamma'_\alpha \to \gamma_\alpha , \ N_\alpha \to \Lambda_\alpha / \gamma_\alpha ,$$
and
$$D'_\alpha \to (\gamma_\alpha + i\Delta)^{-1} , \tag{73}$$

for $\alpha = a, b$, and f_a and f_b are given by Eqs. (28) and (30) without the primes. Furthermore the scattering term S is proportional to $\Lambda_\alpha / \gamma_\alpha$, leading to a contribution $\propto \Lambda_a^2$, and hence can be neglected. This result agrees with Mollow's assertion[28] and Cooper and Ballagh's[29] four-level-model results. In particular, this means that resonant Rayleigh scattering is negligible from a laser with an excited lower state, although not from one with a ground lower state like ruby. With these simplifications, Eqs. (70) and (71) reduce to

$$A_1 = \frac{g^2 D_1}{1 + I_2 L_2} \left[f_a - \frac{I_2 \frac{\gamma}{2} [F D_1 f_a + (N_a - N_b) D_b D_2^* / 2T_1]}{1 + I_2 F \frac{\gamma}{2}(D_1 + D_3^*)} \right] , \tag{74}$$

$$B_1 = \frac{g^2 D_1}{1 + I_2 L_2} \left[f_b - \frac{I_2 \frac{\gamma}{2} [F D_1 f_b + (N_b - N_a) D_a D_2^* / 2T_1]}{1 + I_2 F \frac{\gamma}{2}(D_1 + D_3^*)} \right] . \tag{75}$$

This agrees with the coefficients given in Ref. 22 provided we set $N_b = 0$.

V. THREE-MODE INTERACTIONS

When a third mode at frequency ν_3 is introduced, the density matrix elements of Eqs. (36), (37), and (38) acquire new contributions connecting with the states

$$|0\rangle \equiv |b n_1 + 1 n_2 - 1 n_3 + 1\rangle$$

and

$$|7\rangle \equiv |a n_1 n_2 + 1 n_3 - 1\rangle$$

as shown in Fig. 4. These are, in turn, coupled to the states

$$|6\rangle \equiv |a n_1 + 1 n_2 - 2 n_3 + 1\rangle$$

and

$$|3\rangle \equiv |b n_1 n_2 + 2 n_3 - 1\rangle ,$$

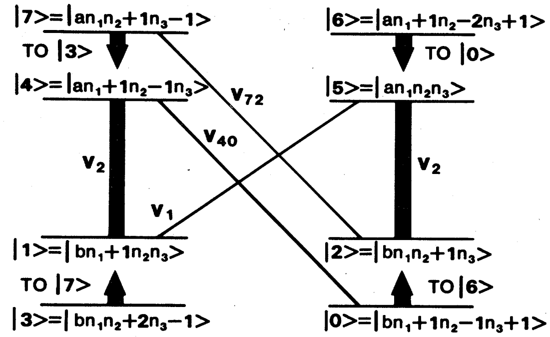

FIG. 4. Eight-level atom-field energy level scheme valid for one strong mode and two-weak side modes. This case treats cavity side-mode instability problems and phase conjugation.

respectively. Again using the Hamiltonian of Eq. (32) with the sum now over all three modes, we find $\dot\rho_{51}$, $\dot\rho_{11}$, and $\dot\rho_{55}$ are the same and the remaining equations of motion become

$$\dot\rho_{54}=-(\gamma_a+\Gamma+i\Delta)\rho_{54}+\Lambda_a\rho_{c010,c100} -i(V_{51}\rho_{14}-\rho_{51}V_{14}+V_{52}\rho_{24})+i\rho_{50}V_{04}\ , \qquad (76)$$

$$\dot\rho_{21}=-(\gamma_b+i\Delta)\rho_{21}+\Gamma\rho_{54}+\Lambda_b\rho_{c010,c100} +i(\rho_{25}V_{51}-V_{25}\rho_{51}+\rho_{24}V_{41})-iV_{27}\rho_{71}\ , \qquad (77)$$

$$\dot\rho_{24}=-(\gamma-i\Delta_3)\rho_{24}-iV_{25}\rho_{54}+i\rho_{21}V_{14} +(i\rho_{20}V_{04}-iV_{27}\rho_{74})\ , \qquad (78)$$

where $V_{04}=gU_3^*\sqrt{n_3+1}$ and $V_{27}=gU_3^*\sqrt{n_3}$. The corresponding equation of motion for the scattering coherence function $\rho_{010,100}$ of Eq. (48) becomes

$$\dot\rho_{010,100}=-i\Delta\rho_{010,100}-iV_1(\rho_{14}-\rho_{25})-iV_{27}\rho_{71}+iV_{04}\rho_{50} \qquad (79)$$

which gives

$$\rho_{101,100}=-\frac{iV_1(\rho_{14}-\rho_{25})+iV_{27}\rho_{71}-iV_{04}\rho_{50}}{i\Delta}\ . \qquad (80)$$

In these equations, ρ_{20}, ρ_{74}, ρ_{50}, and ρ_{71} are multiplied by the weak third-mode interaction energy, and hence they can be calculated in steady state taking into account the strong ν_2 mode alone. They are determined by a calculation very similar to that for the level populations $\rho_{\alpha\alpha}$ and dipoles ρ_{14} and ρ_{25} above, and their steady-state values are given by the single-mode values in Sec. I by one-to-one correspondences. In particular, the ρ_{74} term belongs to a closed set of four terms with the equations of motion

$$\dot\rho_{74}=-(\gamma_a+\Gamma)\rho_{74}+\Lambda_a\rho_{c01-1,c1-10}-iV_{73}\rho_{34}+i\rho_{71}V_{14}\ , \qquad (81)$$

$$\dot\rho_{31}=-\gamma_b\rho_{31}+\Gamma\rho_{74}+\Lambda_b\rho_{c01-1,c1-10}-iV_{37}\rho_{71}+i\rho_{34}V_{41}\ , \qquad (82)$$

$$\dot\rho_{71}=-(\gamma+i\Delta_2)\rho_{71}-iV_{73}\rho_{31}+i\rho_{74}V_{41}\ , \qquad (83)$$

$$\dot\rho_{34}=-(\gamma-i\Delta_2)\rho_{34}-iV_{37}\rho_{74}+i\rho_{31}V_{14}\ . \qquad (84)$$

Here ρ_{74} corresponds to $\rho_{an,an}$ in Eq. (3), ρ_{31} to $\rho_{bn+1,bn+1}$ in Eq. (4), ρ_{71} to $\rho_{an,bn+1}$ in Eq. (5), and ρ_{34} to $\rho_{bn+1,an}$. $\rho_{c01-1,c1-10}$ in Eq. (81) is eliminated similarly to the way $\rho_{cn,cn}$ in Eq. (3) is [see Eqs. (6)–(8)]. The dipole equations (83) and (84) have the steady-state solutions

$$\rho_{34}=-iD_2^*V_2^*(\rho_{74}-\rho_{31})\ , \qquad (85)$$

$$\rho_{71}=iD_2V_2(\rho_{74}-\rho_{31})\ . \qquad (86)$$

With algebra similar to that reaching Eq. (21) for $\rho_{an,an}-\rho_{bn+1,bn+1}$, we find

$$\rho_{74}=N_a\rho_{01-1,1-10}-\frac{2\,|V_2|^2L_2}{\gamma\gamma_a{}'}(\rho_{74}-\rho_{31}) \qquad (87)$$

a similar expression for ρ_{31}, and the difference

$$\rho_{74}-\rho_{31}=\frac{N_a-N_b}{1+I_2L_2}\rho_{01-1,1-10}\ . \qquad (88)$$

Hence in Eqs. (77) and (78) we can substitute

$$\rho_{71}=\frac{iD_2V_2(N_a-N_b)}{1+I_2L_2}\rho_{01-1,1-10}\ . \qquad (89)$$

$$\rho_{74}=\frac{f_a\rho_{01-1,1-10}}{1+I_2L_2}\ . \qquad (90)$$

Similarly the matrix elements ρ_{20}, ρ_{56}, ρ_{50}, and ρ_{26} form a closed set of coupled terms dependent on the field coherence element $\rho_{000,1-21}$. Solving the corresponding equations of motion, we find

$$\rho_{50}=\frac{iD_2V_2(N_a-N_b)}{1+I_2L_2}\rho_{000,1-21}\ , \qquad (91)$$

$$\rho_{20}=\frac{f_b\rho_{000,1-21}}{1+I_2L_2}\ . \qquad (92)$$

Equations (76), (77), and (78) have the steady-state value

$$\rho_{54}=\frac{\Lambda_a\gamma_b\rho_{010,100}D_a'}{\gamma_b+\Lambda_a+\Lambda_b+i\Delta} -iD_a'(V_1\rho_{14}-V_2^*\rho_{51}+V_2\rho_{24}-V_{04}\rho_{50})\ , \qquad (93)$$

$$\rho_{21}=\frac{[(\Lambda_a+\Lambda_b+i\Delta)\Gamma+\gamma_a\Lambda_b]D_b'\rho_{010,100}}{\gamma_a+\Lambda_a+\Lambda_b+i\Delta} +iD_b'(V_1\rho_{25}-V_2^*\rho_{51}+V_2\rho_{24}-V_{27}\rho_{71})\ , \qquad (94)$$

$$\rho_{24}=-iD_3^*[V_2^*(\rho_{54}-\rho_{21})+V_{27}\rho_{74}-V_{04}\rho_{20})]\ . \qquad (95)$$

Combining these with Eq. (80) for $\rho_{010,100}$, we have

$$d_{154}=\rho_{54}-\rho_{21}\,,$$

$$d_{154}=\frac{iV_2^*\rho_{51}F'2T_1-i(D_a'+S/i\Delta)V_1\rho_{14}-i(D_b'-S/i\Delta)V_1\rho_{25}}{1+I_2F\frac{\gamma}{2}(D_1+D_3^*)}+\frac{-V_2(V_{27}\rho_{74}-V_{04}\rho_{20})D_3^*F'2T_1+i(D_a'+S/i\Delta)V_{04}\rho_{50}+i(D_b'-S/i\Delta)V_{27}\rho_{71}}{1+I_2F\frac{\gamma}{2}(D_1+D_3^*)}\,.$$

Substituting values for the ρ_{ij}, we have

$$d_{154}=-V_1V_2^*\frac{F'2T_1d_{051}D_1+(D_a'+S/i\Delta)d_{041}D_2^*+(D_b'-S/i\Delta)d_{052}D_2^*}{1+I_2F\frac{\gamma}{2}(D_1+D_3^*)}-\frac{V_2V_{27}\rho_{01-1,1-10}}{1+I_2L_2}\frac{F'2T_1f_aD_3^*+(N_a-N_b)(D_b'-S/i\Delta)D_2}{1+I_2F\frac{\gamma}{2}(D_1+D_3^*)}+\frac{V_2V_{04}\rho_{000,1-20}}{1+I_2L_2}\frac{F'2T_1f_bD_3^*-(N_b-N_a)(D_a'+S/i\Delta)D_2}{1+I_2F\frac{\gamma}{2}(D_1+D_3^*)}\,. \tag{96}$$

Substituting Eq. (96) into (55) and (49) and tracing over n_3, we find the mode 1 photon-number equation of motion

$$\dot{p}_{n_1}=-(n_1+1)[A_1p_{n_1}-(B_1+\nu/2Q_1)p_{n_1+1}]+n_1[A_1p_{n_1-1}-(B_1+\nu/2Q_1)p_{n_1}]-\sum_{n_3}\sqrt{n_1+1}(C_1\sqrt{n_3}\rho_{01-1,1-10}-D_1\sqrt{n_3+1}\rho_{000,1-21}+\text{c.c.})+\sum_{n_3}\sqrt{n_1}(C_1\sqrt{n_3}\rho_{-11-1,0-10}-D_1\sqrt{n_3+1}\rho_{-100,0-21}+\text{c.c.})\,, \tag{97}$$

where the A_1 and B_1 coefficients are given by Eqs. (65) and (66), and the mode coupling coefficients C_1 and D_1 are given by

$$C_1=-\frac{g^2D_1U_1^*U_3^*V_2^2}{1+I_2L_2}\frac{F'2T_1D_3^*f_a+(N_a-N_b)D_2(D_b'-S/i\Delta)}{1+I_2F\frac{\gamma}{2}(D_1+D_3^*)}\,, \tag{98}$$

$$D_1=-\frac{g^2D_1U_1^*U_3^*V_2^2}{1+I_2L_2}\frac{F'2T_1D_3^*f_b-(N_a-N_b)D_2(D_a'+S/i\Delta)}{1+I_2F\frac{\gamma}{2}(D_1+D_3^*)}\,. \tag{99}$$

Note that for unidirectional equal-frequency operation, the spatial factors U_n in the V's cancel out, and we can replace $4U_1^*U_3^*V_2^2T_1T_2$ by I_2 as for A_1 and B_1. If the mode frequencies differ, a phase mismatch occurs as in the semiclassical case. Similarly for more general orientations, phase matching plays an important role. As discussed below, C_1-D_1 yields the semiclassical coupling coefficient in four-wave mixing.

We can write an operator equation that yields Eq. (97) by noting the matrix elements

$$\sqrt{(n_1+1)n_3}\rho_{01-1,110}=\langle 000\,|\,a_3^\dagger\rho a_1^\dagger\,|\,000\rangle\,,$$

$$\sqrt{(n_1+1)(n_3+1)}\rho_{000,1-21}=\langle 000\,|\,\rho a_1^\dagger a_3^\dagger\,|\,000\rangle\,,$$

$$\sqrt{n_1n_3}\rho_{-11-1,0-10}=\langle 000\,|\,a_1^\dagger a_3^\dagger\rho\,|\,000\rangle\,,$$

$$\sqrt{n_1(n_3+1)}\rho_{-100,0-21}=\langle 000\,|\,a_1^\dagger\rho a_3^\dagger\,|\,000\rangle\,,$$

$$(n_1+1)p_{n_1}=\sum_{n_3}\langle 000\,|\,\rho a_1a_1^\dagger\,|\,000\rangle\,,$$

$$(n_1+1)p_{n_1+1}=\sum_{n_3}\langle 000\,|\,a_1\rho a_1^\dagger\,|\,000\rangle\,,$$

$$n_1p_{n_1-1}=\sum_{n_3}\langle 000\,|\,a_1^\dagger\rho a_1\,|\,000\rangle\,,$$

$$n_1p_{n_1}=\sum_{n_3}\langle 000\,|\,a_1^\dagger a_1\rho\,|\,000\rangle\,.$$

Inserting these into (97) and removing the traces over n_3, we find

$$\dot{\rho}=-A_1(\rho a_1a_1^\dagger-a_1^\dagger\rho a_1)-(B_1+\nu/2Q_1)(a_1^\dagger a_1\rho-a_1\rho a_1^\dagger)+D_1(\rho a_3^\dagger a_1^\dagger-a_1^\dagger\rho a_3^\dagger)+C_1(a_1^\dagger a_3^\dagger\rho-a_3^\dagger\rho a_1^\dagger)+(\text{same with }1\rightarrow 3)+\text{adjoint.} \tag{100}$$

Equation (100) yields the correct semiclassical coupled-mode equations for the mode amplitudes $E_1=\langle a_1\rangle$ and $E_3^*=\langle a_3^\dagger\rangle$, namely

$$\dot{E}_1=\langle a_1\dot{\rho}\rangle=(A_1-B_1-\nu/2Q_1)E_1+(C_1-D_1)E_3^* , \tag{101}$$

$$\dot{E}_3{}^*=\langle a_3^\dagger\dot{\rho}\rangle=(A_3^*-B_3^*-\nu/2Q_3)E_3^*+(C_3^*-D_3^*)E_1 . \tag{102}$$

These semiclassical equations require the choices $\rho a_1 a_1^\dagger$ and $a_1^\dagger a_1\rho$ in Eq. (100) rather than $a_1 a_1^\dagger \rho$ and $\rho a_1 a_1^\dagger$, respectively, alternate choices permitted by the diagonal matrix element $\dot{p}_{n_1}$ in Eq. (97). Equations (101) and (102) can be used for detuned ($\nu_2\neq\omega$) instability studies[10] or in phase conjugation. In semiclassical phase conjugation, C_1-D_1 is the coupling coefficient $i\kappa_1$, with the value [from Eqs. (98) and (99)]

$$i\kappa_1=-\frac{g^2D_1U_1^*U_3^*V_2^2(N_a-N_b)}{1+I_2L_2}\,\frac{F'2T_1(D_2+D_3^*)}{1+I_2F\frac{\gamma}{2}(D_1+D_3^*)} . \tag{103}$$

Furthermore in the limit $\nu_2=\omega$, Eq. (100) yields the coupled photon-number rate equations

$$\frac{d}{dt}\langle n_1\rangle=(A-B-\nu/Q_1)\langle n_1\rangle+(C-D)\langle a_1^\dagger a_3^\dagger\rangle+A , \tag{104}$$

$$\frac{d}{dt}\langle a_1^\dagger a_3^\dagger\rangle=(A-B-\nu/Q_1)\langle a_1^\dagger a_3^\dagger\rangle+(C-D)\langle n_1\rangle+C , \tag{105}$$

in extension of Eq. (67). The choice $\nu_2=\omega$ yields $A_1=A_3^*$, $B_1=B_3^*$, etc. Further we define $A=A_1+A_1^*$, etc. $\langle a_1^\dagger a_3^\dagger\rangle$ is then real and is the quantum version of Lamb's combination tone, responsible for three-mode mode locking [compare E_1 times Eq. (10.48) of Ref. 1]. To lowest nonzero order in a_2, it results from the four-wave mixing process $a_1^\dagger a_3^\dagger a_2^2$, in which two pump ($\nu_2$) photons are annihilated and both a ν_1 and a ν_3 photon are created. The quantum statistics of four-wave mixing can also be studied using Eq. (100). In a recent paper, Reid and Walls[21] considered four-wave mixing with quantum signal and conjugate waves for the degenerate case in which $\nu_1=\nu_2=\nu_3$.

The present paper shows how one strong classical wave and one or two weak quantal side waves interact in a nonlinear two-level medium. The derivation allows the waves to propagate in arbitrary directions, and can be used to treat noise in weak-signal phase conjugation, buildup from quantum noise of side modes in lasers and optical bistability, resonance fluorescence, Rayleigh scattering, and to treat the effects of stimulated emission and phase conjugation on resonance fluorescence as might be found in cavity configurations. Some applications to these problems is given in Ref. 22. Further applications will be presented in subsequent papers.

ACKNOWLEDGMENTS

It is a pleasure to thank Fred Hopf, Pierre Meystre, and Marlan Scully for useful conversations.

The work of M.S. and D.A.H. was supported in part by the United States Office of Naval Research under contract No. N00014-81-K-0754. The work of M.S.Z. was supported in part by the United States Air Force (Office of Scientific Research).

[1]For background theory, see M. Sargent III, M. O. Scully, and W. E. Lamb, Jr., *Laser Physics* (Addison-Wesley, Reading, Mass., 1974).

[2]For a general introduction to laser instabilities and many references to the early literature, see N. B. Abraham, L. A. Lugiato, and L. M. Narducci, J. Opt. Soc. B **2**, 7 (1985). The semiclassical treatment corresponding to the present paper is also given in this issue by S. Hendow and M. Sargent III.

[3]H. Haken, Z. Phys. **190**, 327 (1966).

[4]H. Risken, C. Schmidt, and W. Weidlich, Z. Phys. **194**, 337 (1966).

[5]R. Graham and H. Haken, Z. Phys. **213**, 420 (1968).

[6]H. Risken and K. Nummedal, J. Appl. Phys. **39**, 4662 (1968).

[7]R. Bonifacio and L. A. Lugiato, Lett. Nuovo Cimento **21**, 505 (1978). The relationship to the three-mode semiclassical theory is explained in Ref. 10 and M. Gronchi, V. Benza, L. A. Lugiato, P. Meystre, and M. Sargent III, Phys. Rev. A **24**, 1419 (1981).

[8]H. Haken, Phys. Lett. **53A**, 77 (1975).

[9]R. Graham, Phys. Lett. **58A**, 440 (1976).

[10]S. T. Hendow and M. Sargent III, Opt. Commun. **40**, 385 (1982) and Opt. Commun. **43**, 59 (1982). L. W. Hillman, R. W. Boyd, and C. R. Stroud, Jr., Opt. Lett. **7**, 426 (1982). The role of population pulsations has also been considered by M. Minden and L. W. Casperson, J. Opt. Soc. Am. B (to be published).

[11]N. Bloembergen and Y. R. Shen, Phys. Rev. **133**, A37 (1964) derived the probe absorption coefficient for homogeneously broadened medium subject to a saturator wave of arbitrary intensity. One of the two population pulsation contributions is missing.

[12]S. E. Schwartz and T. Y. Tan, Appl. Phys. Lett. **10**, 4 (1967) derived the single-side-mode coefficient valid to third order in the saturator field amplitude.

[13]B. R. Mollow, Phys. Rev. A **5**, 2217 (1972) derived the single-side-mode absorption coefficient valid to all orders in the saturator intensity.

[14]S. L. McCall, Phys. Rev. A **9**, 1515 (1974) derived the double side-mode absorption coefficient in resonant media valid to all orders in the saturator intensity and including inhomogeneous broadening. The homogeneous-broadening limit agrees with the eigenvalues found in Refs. 2–5.

[15]M. Sargent III, Appl. Phys. **9**, 127 (1976); M. Sargent III, P. E. Toschek, and H. G. Danielmeyer, Appl. Phys. **11**, 55 (1976); and M. Sargent III and P. E. Toschek, Appl. Phys. **11**, 107 (1976) investigate one and two-side-mode interactions for a variety of decay, orientation, and inhomogeneous broadening parameters. This work is summarized in Ref. 16.

[16]M. Sargent III, Phys. Rep. **43C**, 223 (1978).

[17]L. W. Casperson, IEEE J. Quantum Electron. **QE-14**, 756

(1978); Phys. Rev. A **21**, 911 (1980); **23**, 248 (1981).

[18]J. Bentley and N. B. Abraham, Opt. Commun. **41**, 52 (1982).

[19]N. B. Abraham, M. D. Coleman, M. Maeda, and J. C. Wesson, Appl. Phys. B **28**, 169 (1982).

[20]R. Bonifacio and L. A. Lugiato, Phys. Rev. Lett. **40**, 1023 (1978); L. A. Lugiato, Prog. Opt. **21**, 71 (1984). These authors have treated resonance fluorescence in an optical bistability cavity, but do not show how their optical bistability instability grows from spontaneous emission.

[21]M. D. Reid and D. F. Walls, Opt. Commun. **50**, 406 (1984).

[22]M. Sargent III, M. S. Zubairy, and F. DeMartini, Opt. Lett. **8**, 76 (1983).

[23]M. O. Scully and W. E. Lamb, Jr., Phys. Rev. **159**, 208 (1967).

[24]W. E. Lamb, Jr., Phys. Rev. **134**, A1429 (1964).

[25]S. Singh and M. S. Zubairy, Phys. Rev. A **21**, 281 (1980).

[26]B. R. Mollow, Phys. Rev. **188**, 1969 (1969).

[27]C. Cohen-Tannoudji, in *Frontiers in Laser Spectroscopy,* edited by R. Balian, S. Haroche, and S. Liberman (North-Holland, Amsterdam, 1977), Vol. I.

[28]B. R. Mollow, Phys. Rev. A **13**, 758 (1976).

[29]J. Cooper and R. T. Ballagh, Phys. Rev. A **18**, 1302 (1978).

[30]S. Stenholm, D. A. Holm, and M. Sargent III, following paper [Phys. Rev. A **31**, 3124 (1985)].

[31]M. E. Smithers and H. S. Freedhof, J. Phys. B **8**, L209 (1975).